European Journal of Radiology 81 (2012) e363–e369

Contents lists available at SciVerse ScienceDirect

European Journal of Radiology

journal homepage: www.elsevier.com/locate/ejrad

Coronary artery plaques: Cardiac CT with model-based and adaptive-statistical iterative reconstruction technique

Hans Scheffel, Paul Stolzmann, Christopher L. Schlett, Leif-Christopher Engel, Gyöngi Petra Major, Mihály Károlyi, Synho Do, Pál Maurovich-Horvat, Udo Hoffmann*

Cardiac MR PET CT Program, Massachusetts General Hospital and Harvard Medical School, Boston, USA

ARTICLE INFO

Article history:
Received 29 August 2011
Accepted 25 November 2011

Keywords:
Adaptive statistical iterative reconstruction
Model-based iterative reconstruction
CT angiography
Plaque visualization
Image quality

ABSTRACT

Objectives: To compare image quality of coronary artery plaque visualization at CT angiography with images reconstructed with filtered back projection (FBP), adaptive statistical iterative reconstruction (ASIR), and model based iterative reconstruction (MBIR) techniques.

Methods: The coronary arteries of three ex vivo human hearts were imaged by CT and reconstructed with FBP, ASIR and MBIR. Coronary cross-sectional images were co-registered between the different reconstruction techniques and assessed for qualitative and quantitative image quality parameters. Readers were blinded to the reconstruction algorithm.

Results: A total of 375 triplets of coronary cross-sectional images were co-registered. Using MBIR, 26% of the images were rated as having excellent overall image quality, which was significantly better as compared to ASIR and FBP (4% and 13%, respectively, all $p < 0.001$). Qualitative assessment of image noise demonstrated a noise reduction by using ASIR as compared to FBP ($p < 0.01$) and further noise reduction by using MBIR ($p < 0.001$). The contrast-to-noise-ratio (CNR) using MBIR was better as compared to ASIR and FBP (44 ± 19, 29 ± 15, 26 ± 9, respectively; all $p < 0.001$).

Conclusions: Using MBIR improved image quality, reduced image noise and increased CNR as compared to the other available reconstruction techniques. This may further improve the visualization of coronary artery plaque and allow radiation reduction.

1. Introduction

Computed tomography (CT) coronary angiography has excellent sensitivity and good specificity for the detection of coronary artery stenosis when compared with invasive coronary angiography [1–5]. CT coronary angiography does not only provide data about luminal narrowing of the coronary artery tree but also allows the noninvasive characterization of coronary atherosclerotic plaque [6]. Thereby qualitative and quantitative imaging parameters to characterize plaque at CT may be helpful to improve risk stratification in patients with coronary artery disease (CAD) [7]. However, the ability to detect and distinguish the various plaque types with CT is relatively weak [8]. Although CT coronary angiography has been shown to be highly accurate in detection of calcified plaque, various studies have demonstrated limitations in detection of noncalcified plaque [9,10]. This has been linked to the difficulty to establish outer and inner plaque boundary due to the limited contrast resolution, which may have been influenced by the noise of the CT images [6]. Currently, most CT imaging studies have been reconstructed by using the filtered back projection (FBP) technique. An adaptive statistical iterative reconstruction (ASIR) algorithm was developed to help reduce the quantum noise associated with standard convolution reconstruction algorithms [11,12]. Most recently, an algorithm called model-based iterative reconstruction (MBIR) was introduced representing a latest advancement in the field of reconstruction techniques [13]. ASIR is a hybrid method, which updates iterative reconstruction technique on FBP, and MBIR is a raw data based 3-dimensional image reconstruction method, which increases point spread function and thus image resolution. In general, Iterative reconstruction techniques have been found to yield lower noise than the FBP technique [14].

We hypothesized that both ASIR and MBIR are superior to FBP reconstructions in the visualization of coronary artery plaque at CT coronary angiography using qualitative and quantitative imaging parameters in a controlled ex vivo environment. The purpose of this study was to compare the image quality of CT coronary angiography

* Corresponding author at: Cardiac MR PET CT Program, Department of Radiology, Massachusetts General Hospital and Harvard Medical School, 165 Cambridge St, Suite 400, Boston, MA 02144, USA. Tel.: +1 617 634 0239; fax: +1 617 724 4152.
E-mail address: uhoffmann@partners.org (U. Hoffmann).

0720-048X/$ – see front matter © 2011 Elsevier Ireland Ltd. All rights reserved.
doi:10.1016/j.ejrad.2011.11.051

regarding coronary artery plaque visualization in human ex vivo hearts with images reconstructed with FBP, ASIR, and MBIR techniques.

2. Materials and methods

2.1. Study specimens

All procedures were performed in accordance with local and federal regulations and the Declaration of Helsinki. Approval of the local Ethics Committee was obtained. The human donor hearts were retrieved through the International Institute for the Advancement of Medicine (IIAM). IIAM is a non-profit oriented organization, which facilitates the recovery and placement of donated non-transplantable human organs and tissues with researchers. The donor hearts recovered transplantation evaluation, however, the organs deemed unusable or unable to be transplanted mainly due to CAD.

The donor inclusion criteria according to our protocol were male gender, age between 40 and 70 years, and proven CAD. To minimize the prevalence of coronary segments with chronic total occlusion and severe calcification, donors with long standing diabetes mellitus and/or chronic renal failure were excluded from the study. The maximum warm ischemia time was 6 h and the maximum cold ischemia time was 15 h. The fresh donor hearts were transported to our institution in histidinetryptophan-ketoglutarate or University of Wisconsin solution and packed in wet ice. Three isolated donor hearts (the mean age of the donors: 53 years) were acquired and investigated. The cause of death was stroke in two cases and in one case the cause of death was non-natural. CAD was proven in all donor hearts either with catheter coronary angiography or based on the donor's medical history.

2.2. Specimen preparation

As a first step, the ascending aorta was removed in order to provide access to the coronary artery ostia. The right and the left coronary arteries were selectively canulated with plastic luers. The luers were secured in the coronary arteries by ligating the ostial part of the coronaries from the outer surface of the coronary. After implanting the luers in the coronary arteries, a balloon was placed in the left ventricle and inflated with saline to regain the physiological shape of the left ventricle. The following steps were performed on the heart submerged in saline bath. The coronaries were flushed with saline to remove superficial thrombus and air bubbles. As the next step plastic tubes filled with methylcellulose based iodinated contrast agent were attached under water to the luers. The loose ends of the plastic tubes were sealed with a T-port valve. The heart was positioned in the centre of a Styrofoam box filled with canola oil to simulate the epicardial adipose tissue compartment.

2.3. CT protocol

The heart was placed in styrofoam-box on the CT table and methylcellulose based contrast agent (approximately 5–10 ml) was injected in the coronary arteries. To achieve an intra-luminal contrast enhancement similar to in vivo CTA of the coronary arteries a methylcellulose (Methocel, DOW Chemical Company, Midland, MI) with 3% iopamidol contrast agent (Isovue 370, Bracco Diagnostics, Milan, Italy) was used. Typically, with this procedure an attenuation within the vessel lumen was achieved similar to in-vivo studies. All CT data acquisition was performed with a 64-detector row CT scanner (High-Definition, GE Discovery, CT 750HD). The following parameters were used for scanning: 64 mm × 0.625 mm collimation; 0.35 s rotation time; tube voltage of 120 kV; tube current of 500 mAs.

2.4. CT image reconstruction

Iterative reconstruction techniques are an approach to improve the image quality of CT images based on two parts: (1) system optics or geometry (i.e., data fidelity term) and (2) noise statistics (i.e., priori information). In comparison to FBP, iterative reconstruction algorithms are able to synthesize the forward projection for each X-ray projection angle, taking into account the actual process of CT scanning in which X-ray photons originate from their location at a focal spot to the detector through the scanned object. This residual error between this forward projection and the scanner-acquired raw projection data is back-projected to update the image. Furthermore, iterative reconstruction techniques are able to incorporate noise statistical information as a priori information in the mathematic formulation of the reconstruction process.

Thereby, a modeling of the actual detector response function, focal spot size, and system geometry (so called system optics modeling) along with statistical behavior of incident photons and electronic noise (so called statistical modeling) is performed. Unlike the FBP technique, the model-based iterative reconstruction technique synthesizes the forward projection by using dedicated system optics modeling and compares it with the actual measurement. Initial images for model-based iterative reconstruction are filtered back projection-reconstructed images because they are closer to the final results than other assumptions and help to speed up the reconstruction process. This technique also accounts for statistical modeling of the reconstructed object to balance substantial fluctuation of the individual image voxel. These reconstruction steps may help to improve image quality with respect to noise and resolution.

ASIR is a reconstruction algorithm that performs computations to compare image data to a noise model to improve image quality from a perspective that focuses on the modeling of the system noise statistics. Only a limited number of iterations are required to complete an entire analysis for ASIR that was performed at the workstations of our department's CT console. In our study, the average reconstruction time was approximately 40–60% longer with the ASIR algorithm than with the standard FBP reconstruction algorithm.

MBIR is a reconstruction algorithm that is able to improve image quality by modeling the system statistics and the system optics. The MBIR algorithm is more time consuming due to multiple iterations from raw data based image reconstruction. It analyzes the X-ray beam from the focal spot to the shape of the beam as it passes through the patient three-dimensionally and again once more as the beam strikes the X-ray detector on the other side of the patient. Therefore the reconstructions for MBIR data sets were performed outside our department by the vendor (GE, Healthcare) at workstations equipped with dedicated software and computational power to ensure adequate reconstructions.

All Images were reconstructed at 0.625-mm slice thickness with FBP, ASIR, and MBIR techniques by using soft-tissue kernel. All reconstructed CT images were sent to an offline workstation for further analysis.

2.5. Co-registration of the reconstruction techniques

An experienced investigator, who was not participating in the image analysis, performed the matching process. The matched cross-sectional images from all three reconstruction modes were analyzed in one millimeter longitudinal intervals. Multiplanar reformations perpendicular to the vessel centerline were performed in one-millimeter intervals. The CT cross-sectional orientation was based on distance calculations from the coronary ostia and on fiducial markers (side branches, bifurcations and vessel wall morphological features).

2.6. CT data analysis

Image analysis were performed at a commercially available workstation (Advantage Windows 4.2; GE Healthcare) by an cardiac radiology fellow who was blinded to the image review results and had 1 and 2 year of experience in cardiovascular imaging, respectively. The three image sets, obtained with reconstruction techniques FBP, ASIR, and MBIR in each patient, were displayed side by side a preset soft tissue window (window width, 200 HU; window level, 700 HU).

2.7. Qualitative image analysis

The two reviewers were asked to grade the overall image quality on a four-point scale (1 = excellent; 2 = good (minor artifacts); 3 = moderate (considerable artifacts but diagnostic quality); 4 = poor, non-diagnostic). Regarding calcification and blooming artifacts both readers were asked to rate if there is calcification or not and if present a three-point scale was used to qualify blooming artifacts (0 = no blooming; 1 = blooming but lumen clearly visualized; 2 = blooming, no lumen visible).

Image noise was defined as overall graininess or mottle in the coronary artery. It was graded on a four-point scale (1 = no image noise; 2 = average noise; 3 = above average noise; 4 = severe noise).

Image sharpness was evaluated on a five-point scale (0 = extremely poor no definable lumen; 1 = poor severe streaking comprising more than 50% of the vessel lumen; 2 = fair vessel walls may show mild streaking or blurring, but a defined lumen is identifiable; 3 = good coronary walls may be blurred but lumen is clearly discernible and separate from the surrounding fat; 4 = excellent coronary walls are sharp and well-defined with no blurring). Such an assessment scheme was used in a previous study of coronary lumen analysis at CT [15,16].

2.8. Quantitative image analysis

We obtained mean CT attenuation values (in Hounsfield units) for the peri-coronary fat and coronary artery by manually placing circular regions of interest (ROIs) at the same image level. The attenuation of the coronary artery was recorded from a single drawn ROI that was as large as the vessel lumen. For each protocol, image noise was measured as the standard deviation of the pixel values from a circular or ovoid ROI drawn in a homogeneous region of the peri-coronary fat. For all measurements, the size, shape, and position of the ROIs were kept constant among the three protocols by applying a copy and paste function at the workstation. The attenuation of the peri-coronary fat was recorded as the measurement of one ROI placed in the in the peri-coronary area to the coronary lumen. Areas of focal changes in parenchymal attenuation and prominent artifacts, if any, were carefully avoided. For each of the three reconstructions, the contrast-to-noise ratio (CNR) relative to peri-coronary fat for the coronary artery was calculated by using the following equation: $CNR = (HU_{lumen} - HU_{fat})/SD_{lumen}$, where HU_{lumen} and HU_{fat} are the mean CT numbers of the coronary artery lumen and the peri-coronary adipose tissue, respectively. SD_{lumen} represents the SD of luminal CT number.

2.9. Statistical analysis

Continuous variables were expressed as mean ± standard deviation, and categorical variables qualitative parameters as frequencies (percentages). The observer-agreements regarding qualitative parameters (i.e. presence of calcifications, image quality, image noise score, sharpness) between readers and read-outs were analyzed by using weighted kappa and interpreted as follows: a *kappa* value greater than 0.81 corresponded to an excellent agreement and a *kappa* value of 0.61–0.80 corresponded to a good inter-observer agreement. The Mantel-Haenszel Chi^2-test was used to compare categorical parameters between the reconstruction techniques and between images with and without calcifications.

The inter- and intra-reader agreement between quantitative parameters (i.e. luminal CT number, image noise, CNR) was assessed using Pearson's correlation coefficient. Comparisons of quantitative parameters between reconstruction techniques was carried out using ANalysis Of VAriances, *t*-test for related samples was used for pairwise comparisons. Spearman's correlation analysis was used to correlate image noise as assessed quantitatively with the qualitative image noise score. Data analysis was performed using commercially available software (PASW Statistics 18, release 18.0.0, Chicago, IL, USA; SAS, version 9.2 SAS Institute Inc., Cary, NC, USA). A *p*-value of <0.05 was considered statistically significant.

Table 1
Inter- and intra-observer agreement for qualitative parameters.

	Inter-observer		Intra-observer	
	Kappa	Agreement	Kappa	Agreement
Image quality	0.92	>90%	1.00	>90%
Calcification	0.73	85%	0.97	>90%
Blooming	0.47	70%	0.89	>90%
Image noise score	0.62	74%	0.92	>90%
Sharpness	0.38	43%	0.91	>90%

3. Results

A total of 1125 images were derived from all of three datasets reconstructed with FBP, ASIR, and MBIR yielding 375 triples of co-registered image sets. All of these were included in image quality analysis.

3.1. Qualitative image analysis

Kappa-values indicated good to excellent inter- and intra-observer agreement regarding qualitative parameters (Table 1) except for image sharpness ($k = 0.38$). Although both readers had full agreement only in 43% of the cases regarding image sharpness, both were only a single category apart using a 5-point likert scale in 54% of the cases.

Overall image quality was classified to be good or excellent in 274 (73.1%) and 48/375 images (12.8) using FBP, 318 (84.8%) and 15/375 images (4.0%) using ASIR, and 248 (66.1%) and 96/375 (25.6%) using MBIR (Fig. 1). Image quality was significantly better with MBIR than with ASIR ($p < 0.001$) or FBP ($p < 0.001$). ASIR and FBP reconstruction techniques yielded similar image quality ($p = 0.17$).

Calcifications were observed in 369/1125 images (32.8%), no significant differences were discovered among the three reconstruction algorithms (FBP, 33.9%; ASIR, 32.8%; MBIR, 31.7%; $p = 0.53$). Independent of the CT image reconstruction technique, image quality was significantly ($p < 0.001$) worse calcification was present. Regarding images with presence of calcifications, 87/369 images (23.6%) were considered to show no blooming, 267/369 images (72.4%) were considered to have blooming artifacts but allowing luminal visualization, and 15/369 images (4.1%) were considered to have blooming artifacts rendering luminal visualization impossible. No differences among FBR, ASIR, and MBIR were revealed ($p = 0.95$) (Fig. 2a–c).

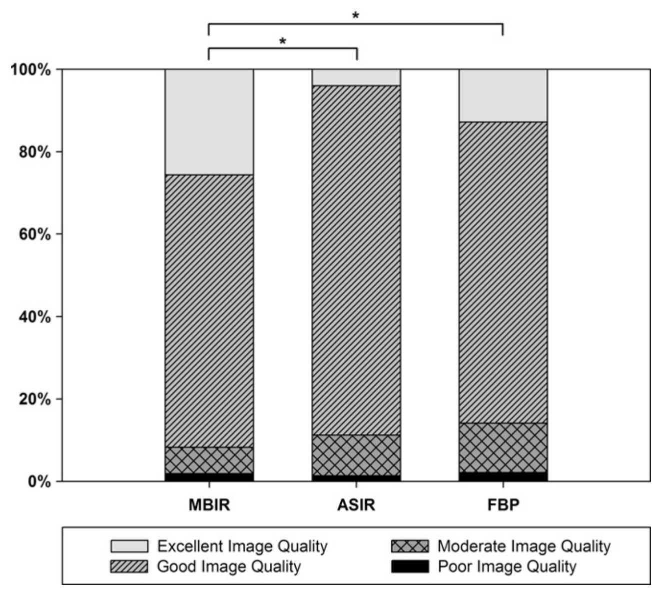

Fig. 1. Overall image quality was significantly better with MBIR than with ASIR ($^{*}p < 0.001$) or FBP ($^{*}p < 0.001$). ASIR and FBP reconstruction techniques yielded similar image quality ($p = 0.17$).

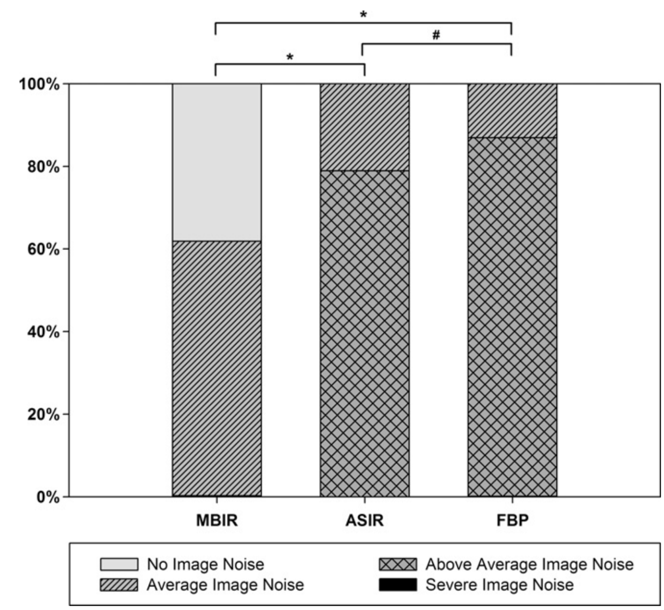

Fig. 3. Image noise score was significantly lower by ASIR as compared to FBP ($^{\#}p < 0.01$) and was further reduced by MBIR as compared ASIR ($^{*}p < 0.001$).

Regarding image noise score the majority of images was rated to be of score 3 using in 325/375 images (86.7%) reconstructed with FBP and in 296/375 images (78.9%) reconstructed with ASIR. Regarding the reconstruction technique of MBIR, images were most frequently classified to be of image noise score 2 representing 231/375 of the cases (61.6%). Image noise was significantly lower by ASIR as compared to FBP ($p < 0.01$) and was further reduced by MBIR as compared ASIR ($p < 0.001$, Fig. 3).

Image sharpness with MBIR was significantly improved with MBIR as compared to ASIR ($p < 0.001$) and FBP ($p < 0.001$); however, ASIR and FBP were comparable ($p = 0.61$). Percentages representing the different image sharpness categories are demonstrated in Figs. 4 and 5a–c according to the individual reconstruction techniques.

3.2. Quantitative image analysis

Inter- and intra-reader correlation coefficients ranged from 0.65 to 0.91 and 0.79 to 0.94, respectively (Table 2). Mean luminal CT number was 297 ± 27 HU and higher (on average 6–10 HU) in images reconstructed with MBIR than in those reconstructed with FBP and ASIR ($p < 0.05$, both; Fig. 6). Mean image noise was 16.0 ± 5.1 HU in images reconstructed with FBP, 14.5 ± 4.3 HU in images reconstructed with ASIR, and 10.2 ± 4.0 HU in images reconstructed with MBIR (Fig. 7). Quantitative assessment of image noise correlated significantly with the qualitative image noise score ($r = 0.43$, $p < 0.001$). Mean CNR was 26 ± 9 HU in images reconstructed with FBP, 29 ± 15 HU in images reconstructed with ASIR, and 44 ± 19 HU in images reconstructed with MBIR (Fig. 8). The image noise and CNR among the three reconstruction techniques were significantly different ($p < 0.001$, both). Image noise was highest using FBP and lowest using MBIR ($p < 0.05$, all); whereas CNR was lowest using FBP and highest using MBIR ($p < 0.05$, all) (see Fig. 8). MBIR increased the CNR by 51–69% while decreasing the noise by 30–36% as compared to both other techniques of ASIR and FBP.

4. Discussion

Our study demonstrates better image quality using MBIR compared with ASIR or FBP for both qualitative and quantitative image analysis. Analysis of ASIR and FBP yielded similar image quality. The

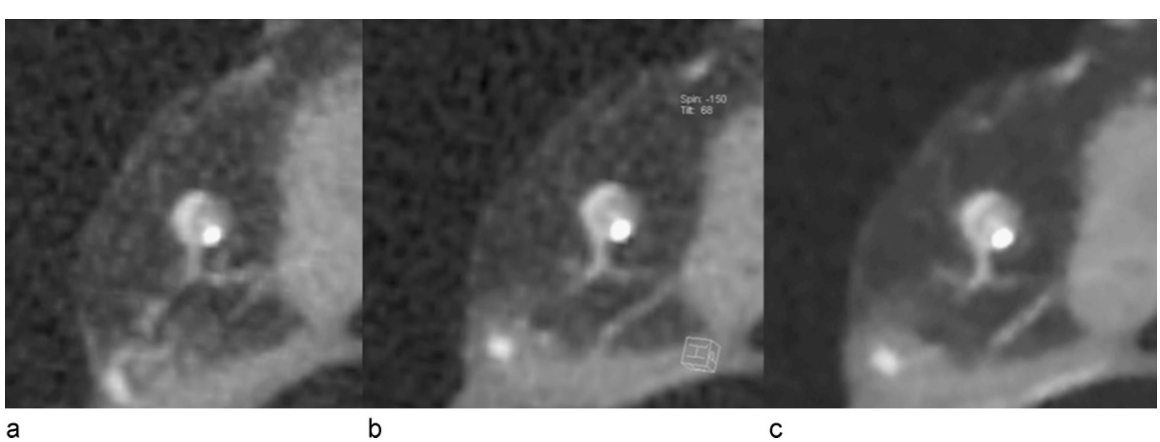

Fig. 2. Cross-sectional CT image reconstructed with (a) FBP, (b) ASIR, and (c) MBIR technique. There is no difference in blooming of calcified component of the coronary artery plaque in the three different reconstruction modes.

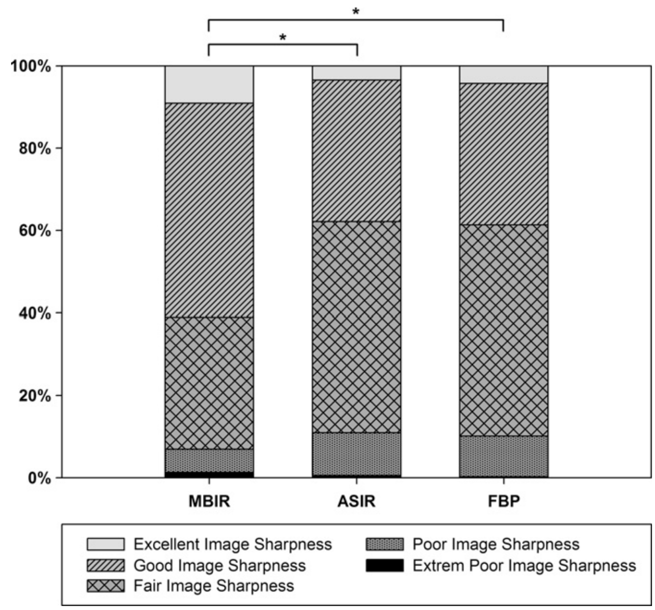

Fig. 4. Image sharpness with MBIR was significantly improved with MBIR as compared to ASIR (* $p < 0.001$) and FBP (* $p < 0.001$); however, ASIR and FBP were comparable (* $p = 0.61$).

image noise was highest using FBP and lowest using MBIR; whereas CNR was lowest using FBP and highest using MBIR. The described MBIR algorithm shows improved image sharpness as compared to ASIR and FBP, but no differences were discovered among the three reconstruction techniques regarding the detection of calcifications. Qualitative image analysis revealed higher mean luminal CT numbers on average in images reconstructed with MBIR than in those reconstructed with FBP and ASIR. The subjective image quality rating for MBIR was better than ASIR and FBP images.

Previous studies that have been evaluated the image quality of iterative reconstructions in chest [11,17] and abdominal [12] CT demonstrated similar results for the comparison of ASIR with FBP. In contrast to their experiences, we were not able to show significant difference regarding the analysis of image quality between ASIR and FBP that was rated equally. This might be related to the use of a subjective overall image quality scoring system. Interestingly Prakash et al. [11] did also found no difference for AISR and FBP for evaluation of small bronchioles of the lungs that was only present when an ASIR-HD reconstruction technique was used. The qualitative rating of image sharpness showed MBIR better than ASIR and FBP images, however, ASIR and FBP were not different. This finding is in line with the findings from overall image quality

Table 2
Inter- and intra-observer correlation for qualitative parameters.

	Inter-observer correlation	Intra-observer correlation
Luminal CT number	0.91	0.94
Image noise	0.82	0.79
CT number of adipose tissue	0.72	0.92

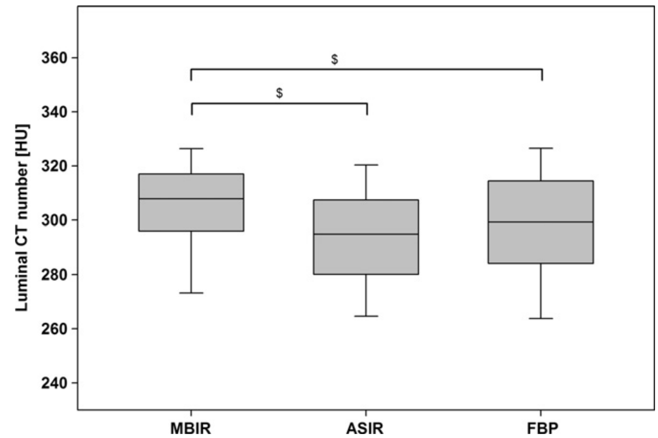

Fig. 6. Mean luminal CT number was 297 ± 27 HU and higher in images reconstructed with MBIR than in those reconstructed with FBP and ASIR ($^{\$}p < 0.05$, both).

reading showing no differences between ASIR and FBP but for MBIR. The coronary image sharpness was assessed subjectively with a considerable inter-observer variability. However, other studies assessing image quality have used similar subjective scoring systems [15,16].

According to our results MBIR and ASIR was not more effective in the suppression of blooming artifacts than FBP at constant X-ray tube settings. We hypothesized, that iterative reconstruction techniques would substantially lower blooming artifacts, enabling better appreciation of the vessel lumen, which have traditionally been recognized as limitation of cardiac CT. However, independent of the CT image reconstruction technique, image quality was significantly worse when calcification was present.

The quantitative analysis showed lower image noise using MBIR compared with ASIR or FBP. We are unable to compare results of our study owing to lack of published clinical studies of the MBIR technique. However, prior phantom studies using the MBIR techniques for CT image reconstruction have reported potential for image noise and artifact reduction [13,18,19]. Thus, lower image noise with the

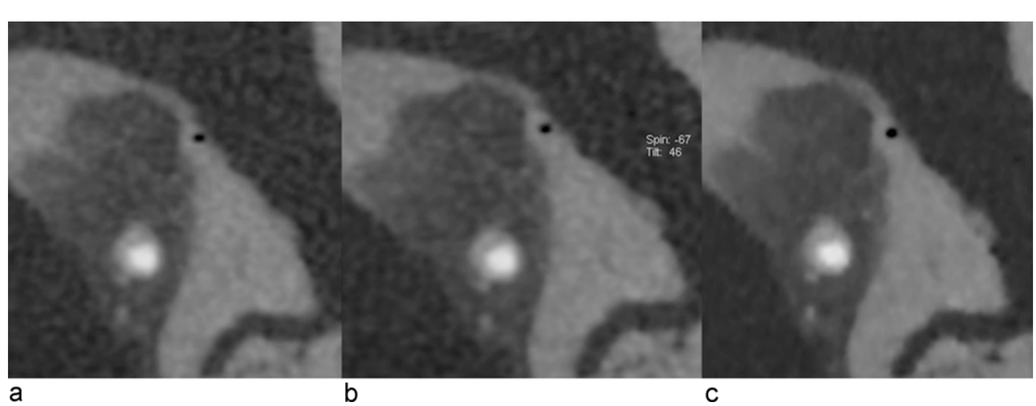

Fig. 5. Cross-sectional CT image reconstructed with (a) FBP, (b) ASIR, and (c) MBIR technique. Note the substantial reduction in noise better sharpness vessel lumen and adjacent vessel wall in (c) compared with (a) and (b).

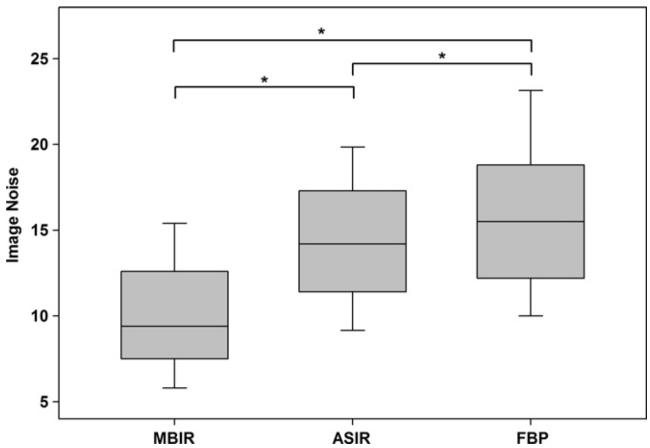

Fig. 7. The three reconstruction techniques were significantly different for image noise ($^{*}p < 0.001$).

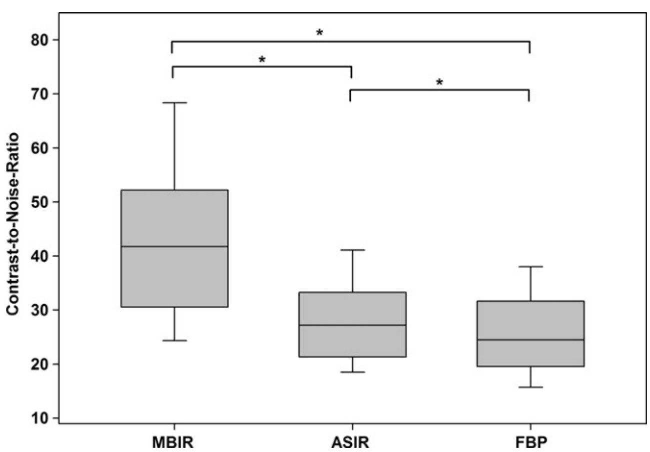

Fig. 8. The three reconstruction techniques were significantly different for contrast-to-noise-ratio (CNR) ($^{*}p < 0.001$).

MBIR and ASIR reconstruction techniques allow the use of sharper or greater edge-enhancement kernels, which may have contributed to the improved CNR ratio and aided in the visualization of small structures not satisfactorily evaluable with the more noise-prone filtered back projection technique. That ASIR technique is able to lower the images noise has already been found in several other non-coronary CT studies [11,12,14,17,20]. Furthermore, an increase in CNR as in our study was also shown by an abdominal CT study evaluating the potential radiation dose reductions potentially related with this technique [12]. The finding of lower noise and higher CNR together with better vessel sharpness using MBIR compared with ASIR or FBP analysis may have an important clinical implication for the evaluation of coronary artery plaques that needs to be validated in vivo. Qualitative image analysis revealed higher mean luminal CT numbers on average in images reconstructed with MBIR than in those reconstructed with FBP and ASIR. This can be explained by a narrower point spread function.

4.1. Limitations

Several potential limitations of our study merit consideration: first, although we observed significant differences in our results, this investigation reflects our preliminary experience from an ex vivo study on a small number of highly selected coronary arteries. Ex vivo plaque constituents may not be representative of there in vivo equivalents. Second, coronary image sharpness was assessed subjectively, which introduces the possibility of bias into the study. Third, we did not evaluate potential radiation dose saving methods. Owing to increasing concern about the possible radiological–biological consequences of greater cumulative radiation doses from medical exposures, noise efficient reconstruction algorithms such as ASIR should be implemented to reduce radiation doses in cardiac CT protocols. Fourth, the CNR relative to the pericoronary fat represents a surrogate measure of CT image quality that may not completely encompass all of the components needed to make a correct diagnosis. As such, it remains to be determined whether the increase in CNR achieved with MBIR and ASIR markedly increase coronary plaque evaluation. Fifth, high computational cost and long reconstruction times of MBIR remain as a barrier to the use of MBIR in practical applications.

5. Conclusion

In summary, our initial results suggest that use of MBIR algorithm, as compared with ASIR and a standard FBP reconstruction algorithm, leads to significantly improved image quality accompanied with a substantial decrease in image noise and increase of the CNR. These findings and the ability to achieve better vessel sharpness using MBIR compared with ASIR or FBP may have an important clinical implication in the evaluation of the coronary artery tree that needs to be validated in vivo.

6. Disclosure

This study was partially funded by an unrestricted research grant of GE Healthcare.

Acknowledgement

We would like to thank you GE Healthcare for supporting our work with access to pre-commercial model-based reconstruction techniques.

References

[1] Ferencik M, Chan RC, Achenbach S, Lisauskas JB, Houser SL, Hoffmann U, et al. Arterial wall imaging: evaluation with 16-section multidetector CT in blood vessel phantoms and ex vivo coronary arteries. Radiology 2006;240(3):708–16.
[2] Hoffmann U, Moselewski F, Nieman K, Jang IK, Ferencik M, Rahman AM, et al. Noninvasive assessment of plaque morphology and composition in culprit and stable lesions in acute coronary syndrome and stable lesions in stable angina by multidetector computed tomography. J Am Coll Cardiol 2006;47(8):1655–62.
[3] Hoffmann U, Nagurney JT, Moselewski F, Pena A, Ferencik M, Chae CU, et al. Coronary multidetector computed tomography in the assessment of patients with acute chest pain. Circulation 2006;114(21):2251–60.
[4] Leber AW, Johnson T, Becker A, von Ziegler F, Tittus J, Nikolaou K, et al. Diagnostic accuracy of dual-source multi-slice CT-coronary angiography in patients with an intermediate pretest likelihood for coronary artery disease. Eur Heart J 2007;28(19):2354–60.
[5] Leschka S, Alkadhi H, Plass A, Desbiolles L, Grunenfelder J, Marincek B, et al. Accuracy of MSCT coronary angiography with 64-slice technology: first experience. Eur Heart J 2005;26(15):1482–7.
[6] Leber AW, Knez A, von Ziegler F, Becker A, Nikolaou K, Paul S, et al. Quantification of obstructive and nonobstructive coronary lesions by 64-slice computed tomography: a comparative study with quantitative coronary angiography and intravascular ultrasound. J Am Coll Cardiol 2005;46(1):147–54.
[7] Leber AW, Becker A, Knez A, von Ziegler F, Sirol M, Nikolaou K, et al. Accuracy of 64-slice computed tomography to classify and quantify plaque volumes in the proximal coronary system: a comparative study using intravascular ultrasound. J Am Coll Cardiol 2006;47(3):672–7.
[8] Leber AW, Knez A, Becker A, Becker C, von Ziegler F, Nikolaou K, et al. Accuracy of multidetector spiral computed tomography in identifying and differentiating the composition of coronary atherosclerotic plaques: a comparative study with intracoronary ultrasound. J Am Coll Cardiol 2004;43(7):1241–7.
[9] Schmermund A, Baumgart D, Gorge G, Seibel R, Gronemeyer D, Ge J, et al. Coronary artery calcium in acute coronary syndromes: a comparative study of electron-beam computed tomography, coronary angiography, and intracoronary ultrasound in survivors of acute myocardial infarction and unstable angina. Circulation 1997;96(5):1461–9.

[10] Knez A, Becker C, Becker A, Leber A, White C, Reiser M, et al. Determination of coronary calcium with multi-slice spiral computed tomography: a comparative study with electron-beam CT. Int J Cardiovasc Imaging 2002;18(4):295–303.
[11] Prakash P, Kalra MK, Ackman JB, Digumarthy SR, Hsieh J, Do S, et al. Diffuse lung disease: CT of the chest with adaptive statistical iterative reconstruction technique. Radiology 2010;256(1):261–9.
[12] Marin D, Nelson RC, Schindera ST, Richard S, Youngblood RS, Yoshizumi TT, et al. Low-tube-voltage, high-tube-current multidetector abdominal CT: improved image quality and decreased radiation dose with adaptive statistical iterative reconstruction algorithm – initial clinical experience. Radiology 2010;254(1):145–53.
[13] Yu Z, Thibault J, Bouman C, Sauer K, Hsieh J. Fast model-based X-ray CT reconstruction using spatially non-homogeneous ICD optimization. IEEE Trans Image Process 2011;20(1):161–75.
[14] Prakash P, Kalra MK, Kambadakone AK, Pien H, Hsieh J, Blake MA, et al. Reducing abdominal CT radiation dose with adaptive statistical iterative reconstruction technique. Invest Radiol 2010;45(4):202–10.
[15] Araoz PA, Kirsch J, Primak AN, Braun NN, Saba O, Williamson EE, et al. Optimal image reconstruction phase at low and high heart rates in dual-source CT coronary angiography. Int J Cardiovasc Imaging 2009;25(8): 837–45.
[16] Weustink AC, Mollet NR, Pugliese F, Meijboom WB, Nieman K, Heijenbrok-Kal MH, et al. Optimal electrocardiographic pulsing windows and heart rate: effect on image quality and radiation exposure at dual-source coronary CT angiography. Radiology 2008;248(3):792–8.
[17] Yanagawa M, Honda O, Yoshida S, Kikuyama A, Inoue A, Sumikawa H, et al. Adaptive statistical iterative reconstruction technique for pulmonary CT: image quality of the cadaveric lung on standard- and reduced-dose CT. Acad Radiol 2010;17(10):1259–66.
[18] Thibault JB, Sauer KD, Bouman CA, Hsieh J. A three-dimensional statistical approach to improved image quality for multislice helical CT. Med Phys 2007;34(11):4526–44.
[19] Ziegler A, Kohler T, Proksa R. Noise and resolution in images reconstructed with FBP and OSC algorithms for CT. Med Phys 2007;34(2):585–98.
[20] Prakash P, Kalra MK, Digumarthy SR, Hsieh J, Pien H, Singh S, et al. Radiation dose reduction with chest computed tomography using adaptive statistical iterative reconstruction technique: initial experience. J Comput Assist Tomogr 2010;34(1):40–5.